Complementary Acid Site Mechanisms in Hydrogen-Free Polyethylene Upcycling: Elucidating the Distinct Roles of Brønsted and Lewis Sites in Ce-Modified Zeolites

Taeeun Kwon [a,b], Jonghyun Park [a], Ki Hyuk Kang [c], Dae Sung Jung [d], Wangyun Won [b,*], Insoo Ro [a,*]

[a] Department of Chemical and Biological Engineering, Korea University, Seoul 02841, Republic of Korea

[b] Department of Chemical and Biomolecular Engineering, Seoul National University of Science and Technology, Seoul 01811, Republic of Korea

[c] Chemical & Process Technology Division, Korea Research Institute of Chemical Technology (KRICT), Daejeon 34114, Republic of Korea

[d] Hyundai Motor Company, Jangduk-ri 772-1, Hwaseong-si, Gyeonggi-do 18280, Republic of Korea

[*]*Corresponding Authors:*

Prof. W. Won (wwon@korea.ac.kr) and Prof. I. Ro (insoo@seoultech.ac.kr)

Table S1. ICP-OES results

Sample	Si (ppm)	Al (ppm)	Metal (ppm)
Na_micro_Y	137,999	83,294	Na: 61,693
Na_meso_Y	106,514	85,850	Na: 66,933
Li_meso_Y	155,826	113,825	Li: 11,208
K_meso_Y	173,405	108,048	K: 94,584
H_Y	197,476	98,867	
La_meso_Y	144,671	87,553	La: 79,521
Ce_meso_Y	105,177	80,731	Ce: 110,850
Ce/HY-WI	179,937	126,431	Ce: 110,527
Ce_meso_Y-0.1	164,044	118,096	Ce: 42,424
Ce_meso_Y-0.3	178,159	123,424	Ce: 148,536
La_meso_Y-0.3	163,654	138,763	La: 119,710

Table S2. Drying results of PE and ISTD in a vacuum oven at 80°C for 48 hours under various conditions

CH_2Cl_2 (mL)	PE (g)	ISTD (g)	Vial before drying (g)	Vial after drying (g)	Weight difference (g)
20	-	-	33.6434	33.6499	0.0065
20	-	0.0351	34.2697	34.2765	0.0068
20	0.4027	-	34.1167	34.5252	0.4085
20	0.1012	0.0381	33.8524	33.9605	0.1081
20	0.2016	0.0350	33.8094	34.0130	0.2036
20	0.4017	0.0374	33.8387	34.2523	0.4136
20	0.6005	0.0365	34.2436	34.8574	0.6138

Table S3. GC-FID compound identification table.

Entry	Name	Category	Retention time (min)
1	iso-Pentane	iso-Alkane	3.4
2	n-Pentane	n-Alkane	3.6
3	Methylene Chloride	(Solvent)	3.8 – 3.9
4	iso-Hexane	iso-Alkane	4.5 – 4.7
5	n-Hexane	n-Alkane	5.0
6	Methylcyclopentane	Cycloalkane	5.6
7	Benzene	Aromatic	6.1
8	Cyclohexane	Cycloalkane	6.3
9	iso-Heptane	iso-Alkane	6.7 – 7.0
10	n-Heptane	n-Alkane	7.3
11	Methylcyclohexane	Cycloalkane	8.0
12	Toluene	Aromatic	9.1
13	iso-Octane	iso-Alkane	9.4 – 9.7
14	n-Octane	n-Alkane	10.5
15	Ethylcyclohexane	Cycloalkane	11.7
16	Ethylbenzene	Aromatic	12.3
17	p-, m-Xylene	Aromatic	12.7
18	iso-Nonane	iso-Alkane	12.8 – 13.1
19	o-Xylene	Aromatic	13.5
20	n-Nonane	n-Alkane	14.0
21	n-Decane	n-Alkane	17.5
22	n-Undecane	n-Alkane	20.7
23	n-Dodecane	n-Alkane	23.7
24	n-Tridecane	n-Alkane	26.6
25	n-Tetradecane	n-Alkane	29.3
26	n-Pentadecane	n-Alkane	31.8
27	n-Hexadecane	n-Alkane	34.2
28	n-Heptadecane	n-Alkane	36.4
29	n-Octadecane	n-Alkane	38.5
30	n-Nonadecane	n-Alkane	40.6
31	n-Eicosane	n-Alkane	42.6
32	n-Heneicosane	n-Alkane	44.4
33	n-Docosane	n-Alkane	46.2

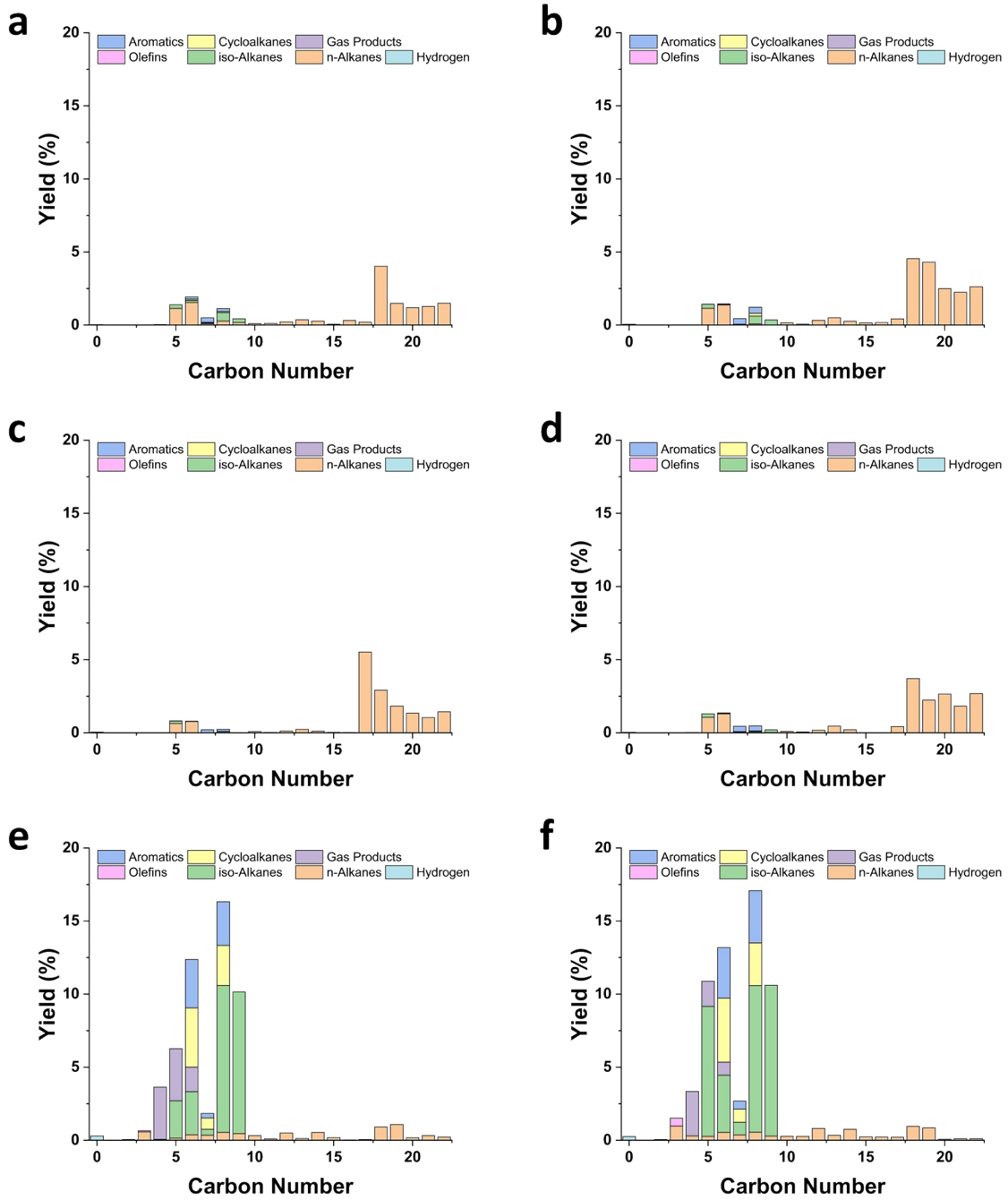

Figure S1. Product distribution from PE catalytic cracking over various zeolites: (a) Na_micro_Y, (b) Na_meso_Y, (c) Li_meso_Y, (d) K_meso_Y, (e) H_Y, and (f) La_meso_Y. Reaction conditions: 300°C, 4 h, atmospheric Ar, 0.1 g catalyst, and 0.2 g PE.

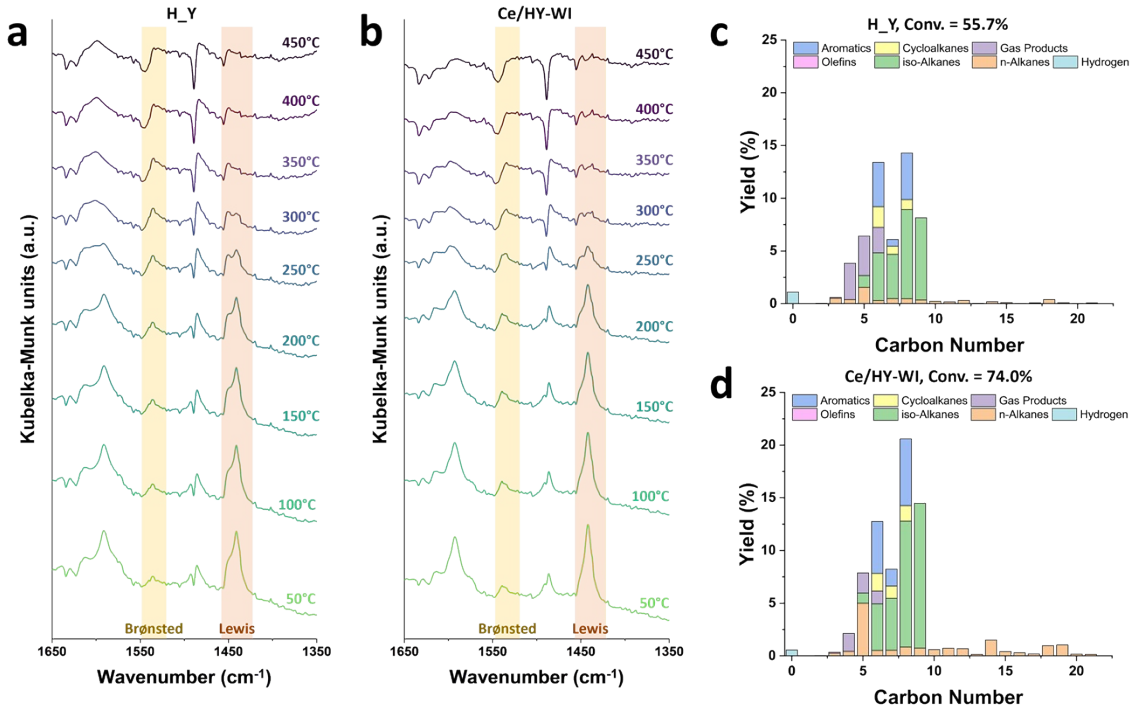

Figure. S2 (a-b) Pyridine-DRIFTS spectra of HY and Ce/HY-WI catalysts after calcination at 550°C for 6 hours at different desorption temperatures. (a) HY and (b) Ce/HY-WI. (c-d) Reaction results of HY and Ce/HY-WI catalysts after calcination at 550°C for 6 hours. (c) HY and (d) Ce/HY-WI. Reaction conditions: 300°C, 2 h, atmospheric Ar, 0.1 g catalyst, and 0.2 g PE.

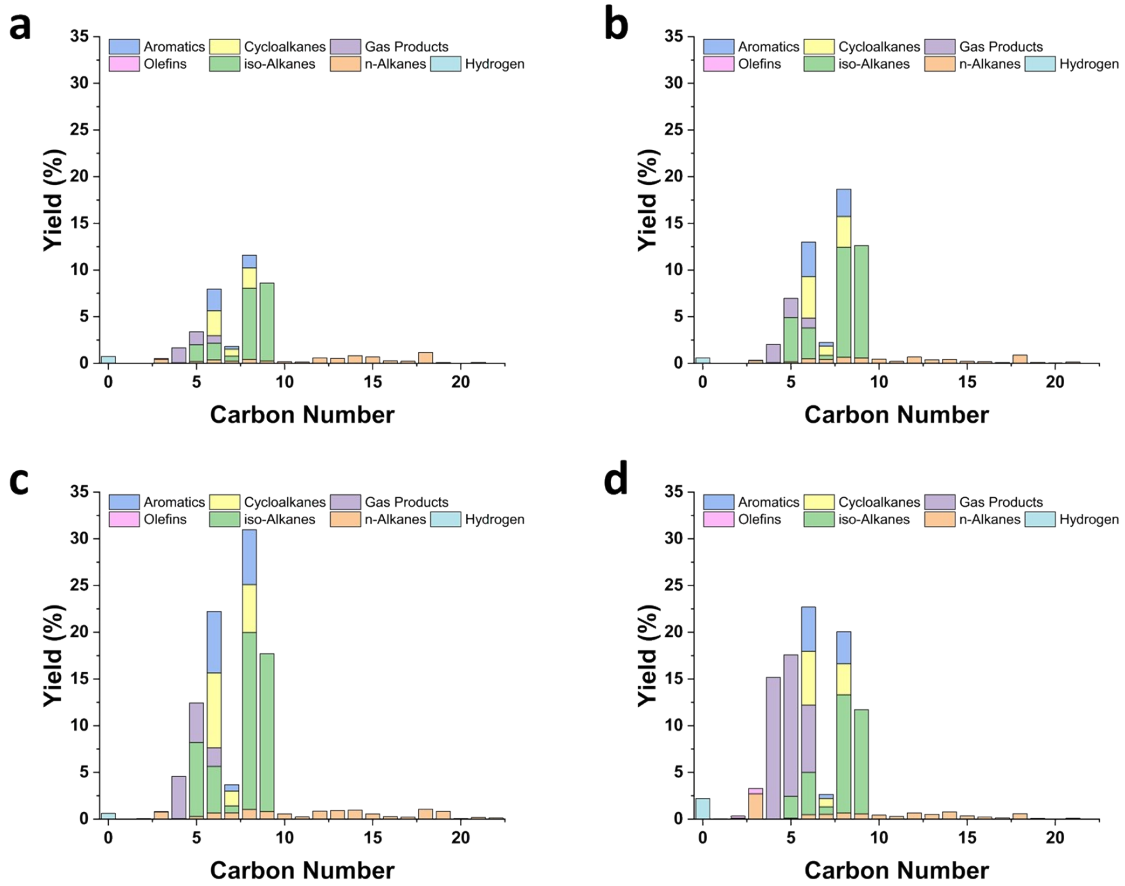

Figure S3. Product distribution from PE catalytic cracking over Ce_meso_Y as a function of reaction temperature. (a) 260 °C, (b) 280 °C, (c) 300 °C, and (d) 320 °C. Reaction conditions: 4 h, atmospheric Ar, 0.1 g catalyst, and 0.2 g PE.

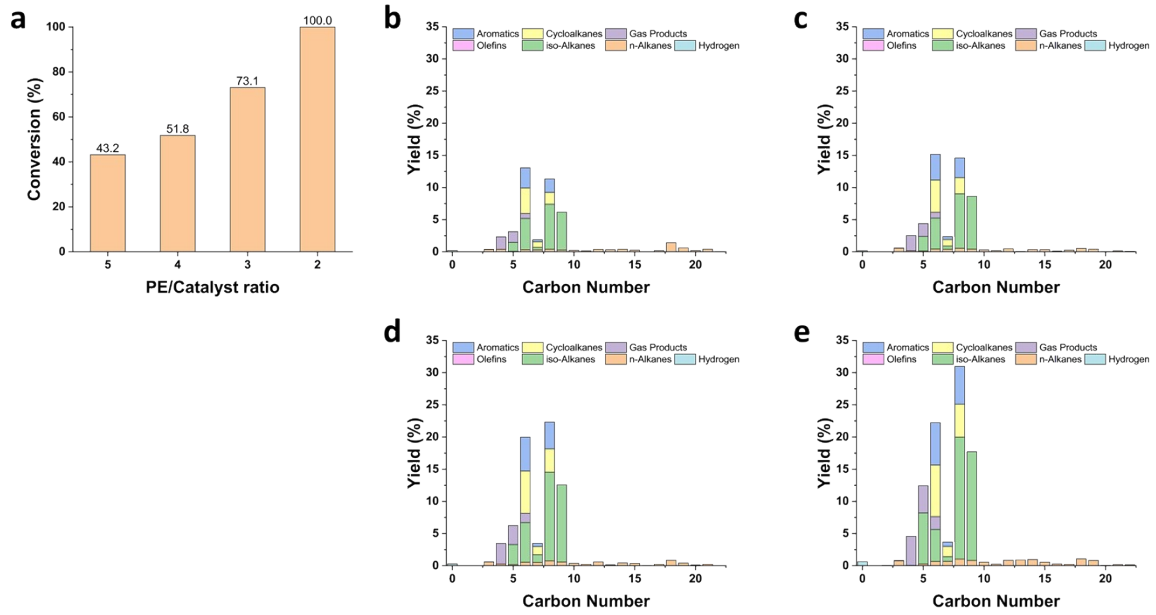

Figure S4. Product distribution from PE catalytic cracking over Ce_meso_Y as a function of PE/Catalyst ratio. (a) Conversion as a function of PE/Catalyst ratio. Product distributions at PE/Catalyst ratio of (b) 5, (c) 4, (d) 3, and (e) 2. Reaction conditions: 300 °C, 4 h, atmospheric Ar, and 0.1 g catalyst.

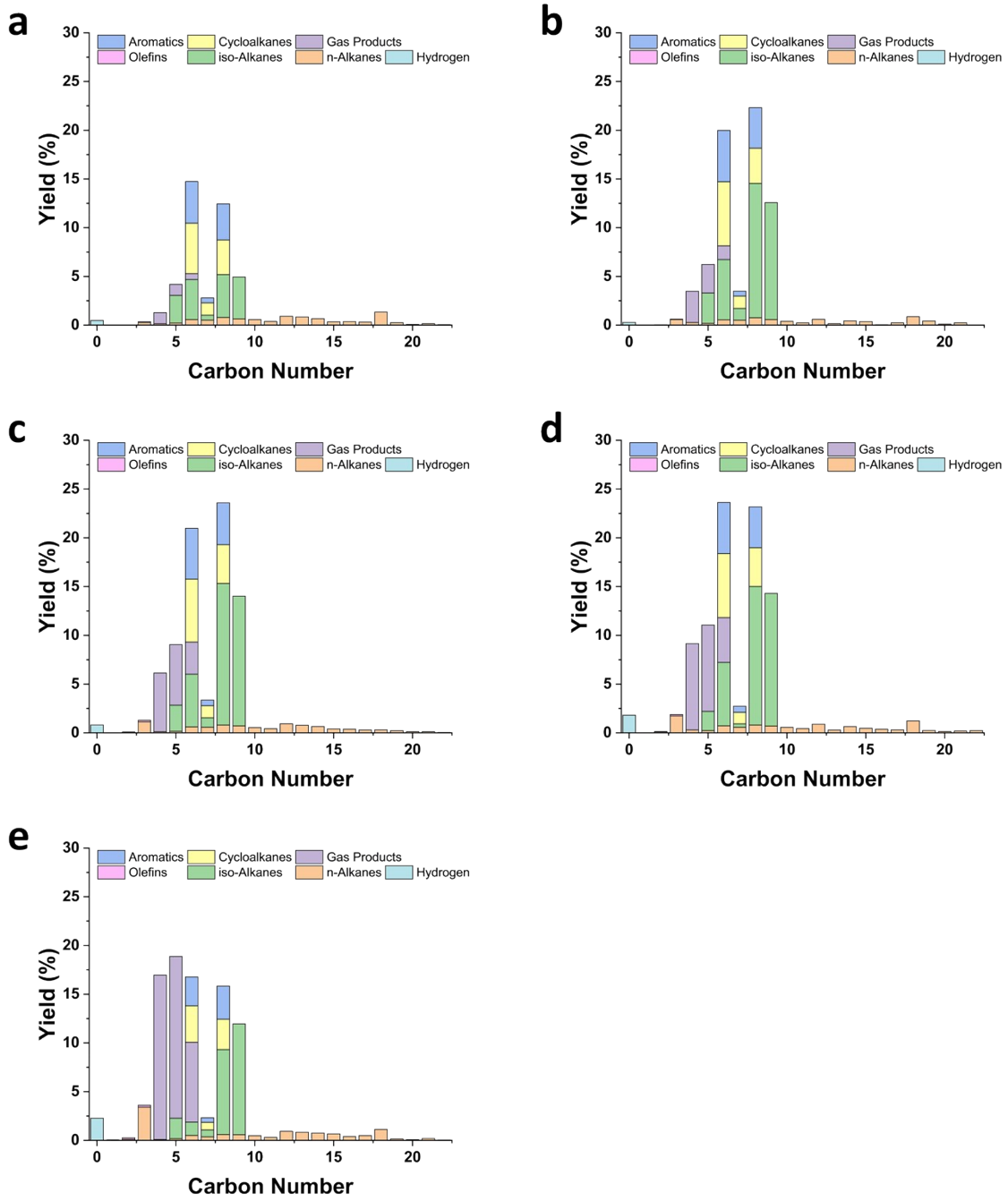

Figure S5. Product distribution from PE catalytic cracking over Ce_meso_Y as a function of reaction time. (a) 2 h, (b) 4 h, (c) 8 h, (d) 16 h, and (e) 24 h. Reaction conditions: 300 °C, atmospheric Ar, 0.1 g catalyst, and 0.3 g PE.

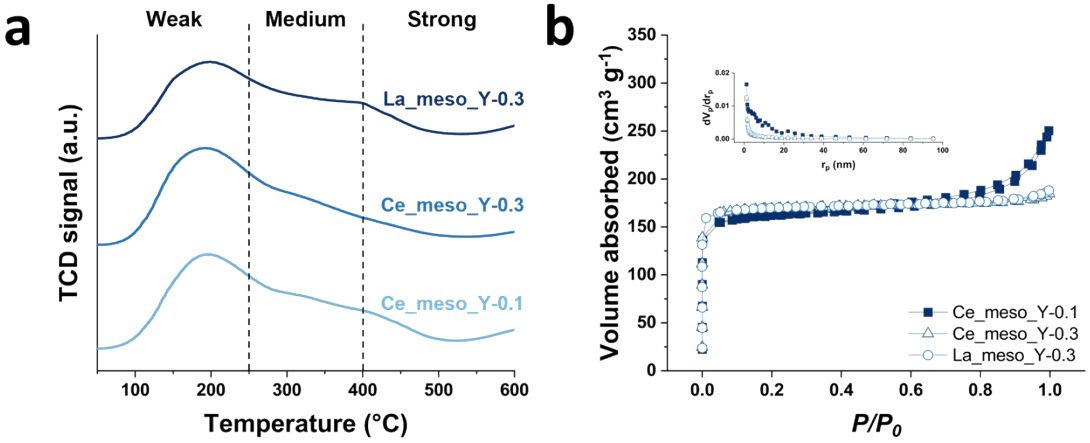

Figure S6. Physicochemical characterization of Ce_meso_Y and La_meso_Y with different loading. (a) NH_3-TPD profile, and (b) N_2 adsorption-desorption isotherms and BJH pore size distribution of zeolites.

Table S4. Catalytic characterization results of different ion-exchanged zeolites.

Catalyst	[a] Surface area ($m^2\ g^{-1}$)	[b] Pore volume ($cm^3\ g^{-1}$)	[c] Acid site density (%)			[c] Total acid site density (mmol $NH_3\ g^{-1}$)
			Weak (50-250 °C)	Medium (250-400 °C)	Strong (400-600 °C)	
Ce_meso_Y-0.1	491	0.376	48.2	35.8	16.0	1.53
Ce_meso_Y-0.3	436	0.282	53.5	33.7	12.9	1.66
La_meso_Y-0.3	451	0.288	49.4	36.6	14.0	1.42

[a] BET surface area evaluated using the standard multipoint method at $P/P_0 = 0.05–0.3$. [b] Total pore volume at $P/P_0 = 0.995$, and [c] Acid site density determined by NH_3-TPD analysis.

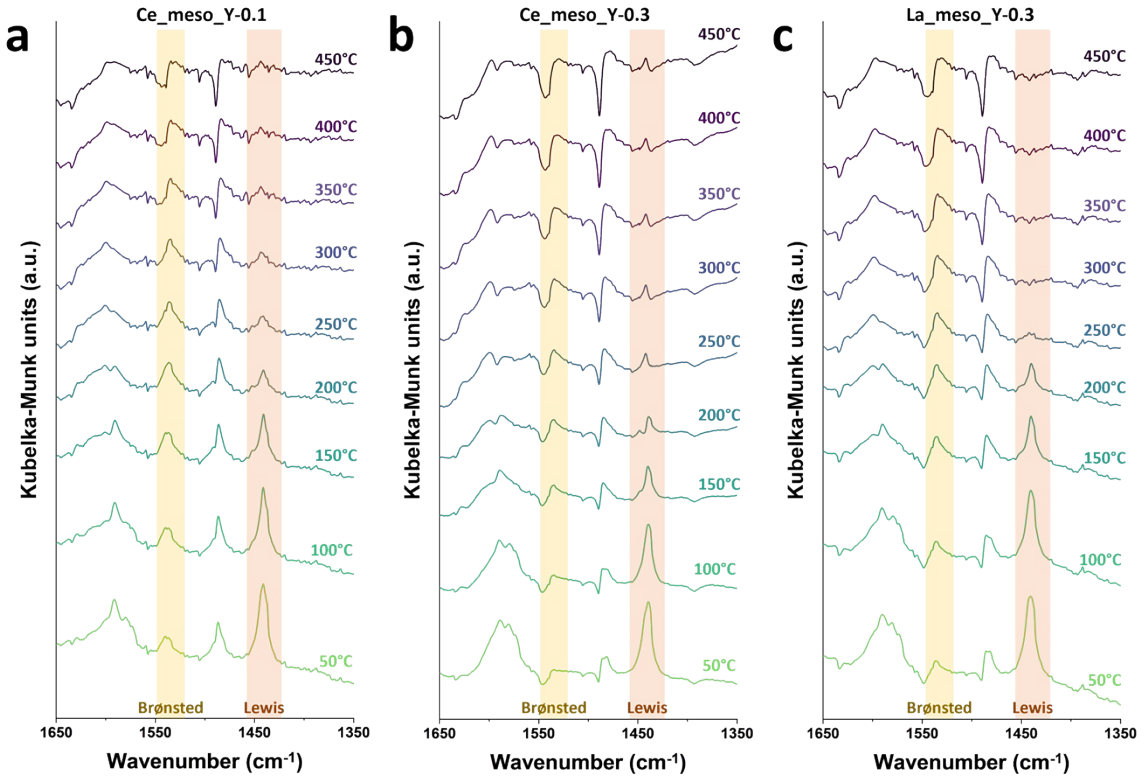

Figure S7. Pyridine-DRIFTS spectra at different desorption temperatures. (a) Ce_meso_Y-0.1 (b) Ce_meso_Y-0.3, and (c) La_meso_Y-0.3.

Table S5. Pyridine-DRIFTS analysis results of Brønsted and Lewis acid sites at different desorption temperatures.

Catalyst	At 50 °C			At 300 °C			At 450 °C		
	BAS (%)	LAS (%)	BAS/LAS	BAS (%)	LAS (%)	BAS/LAS	BAS (%)	LAS (%)	BAS/LAS
Ce_meso_Y-0.1	39.5	60.5	0.652	74.8	25.2	2.965	77.7	22.3	3.479
Ce_meso_Y-0.3	29.7	70.3	0.422	89.6	10.4	8.620	81.3	18.7	4.344
La_meso_Y-0.3	42.4	57.6	0.735	90.8	9.2	9.833	91.0	9.0	10.061

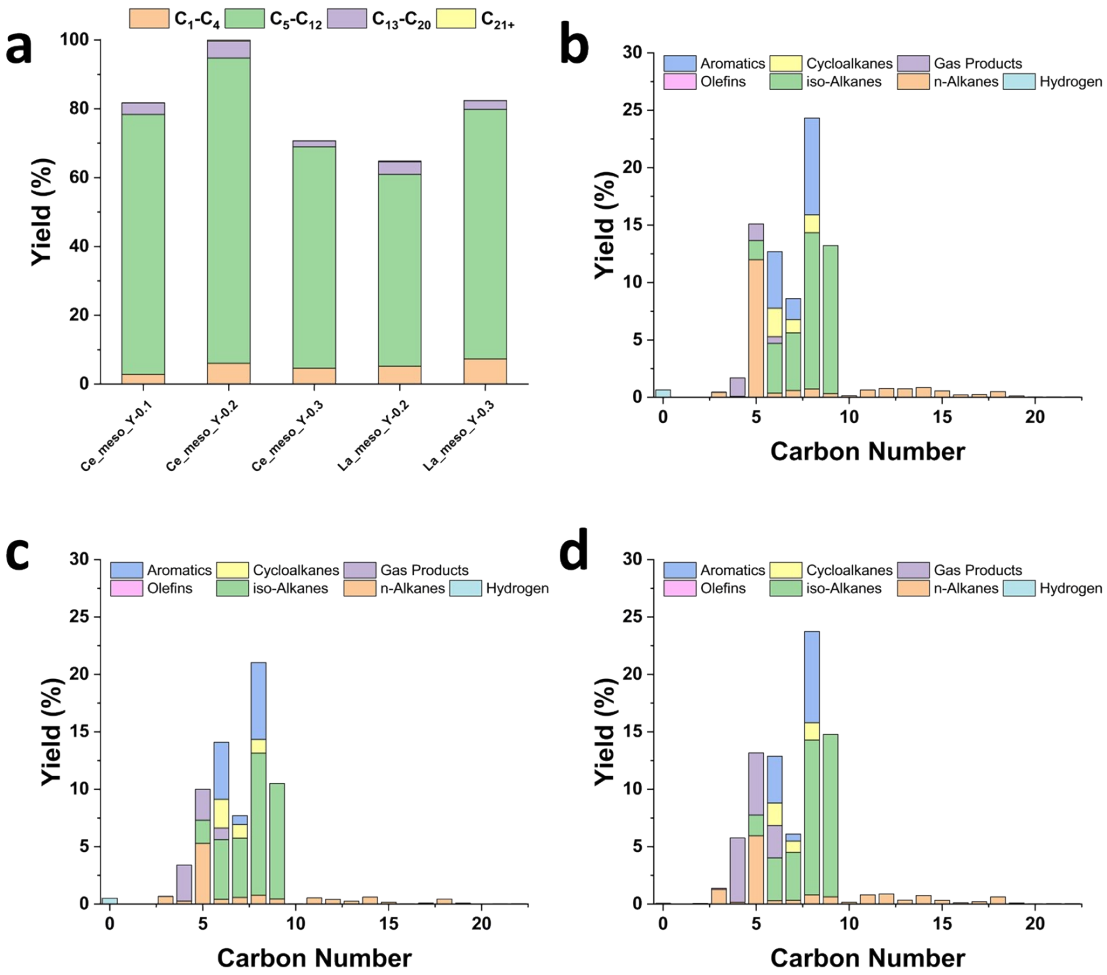

Figure S8. PE catalytic cracking results over Ce_meso_Y and La_meso_Y with different loading. (a) Product yield, (b-d) Product distribution from PE catalytic cracking over (b) Ce_meso_Y-0.1 (c) Ce_meso_Y-0.3, and (d) La_meso_Y-0.3. Reaction conditions: 300°C, 4 h, atmospheric Ar, 0.1 g catalyst, and 0.2 g PE.

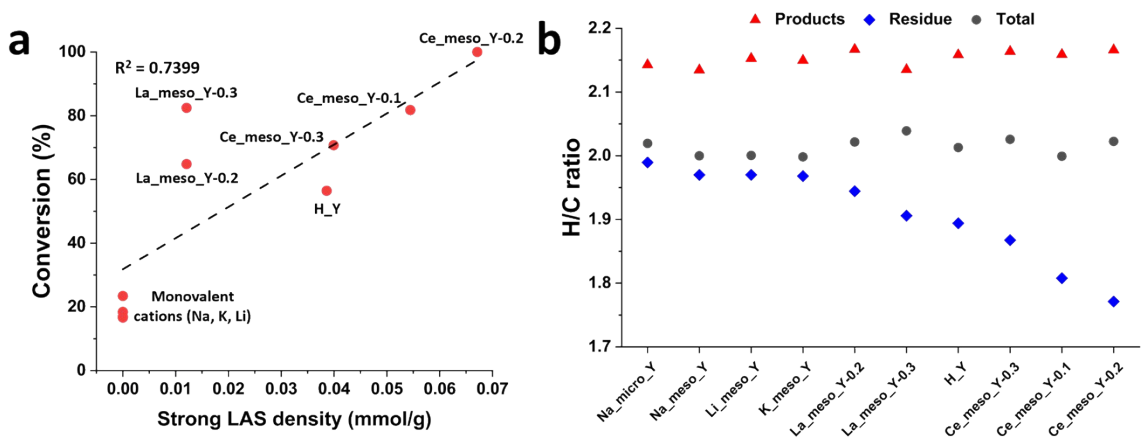

Figure S9. (a) Conversion as a function of strong Lewis acid sites (LASs) density. (b) H/C ratio of products and residues over ion-exchanged zeolites.

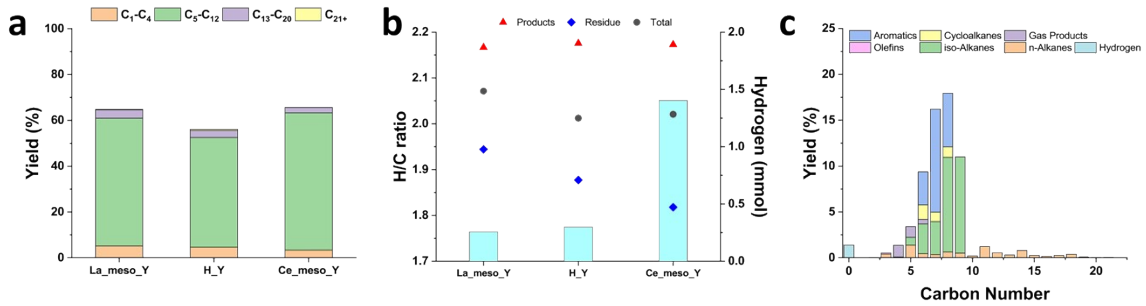

Figure S10. (a) PE catalytic cracking results of different ion-exchanged zeolites. (b) Comparison of H/C ratio and hydrogen yield at similar conversion levels. (c) Product distribution from PE catalytic cracking over Ce_meso_Y. Reaction conditions: 300°C, 2 h, atmospheric Ar, 0.1 g catalyst, and 0.2 g PE.

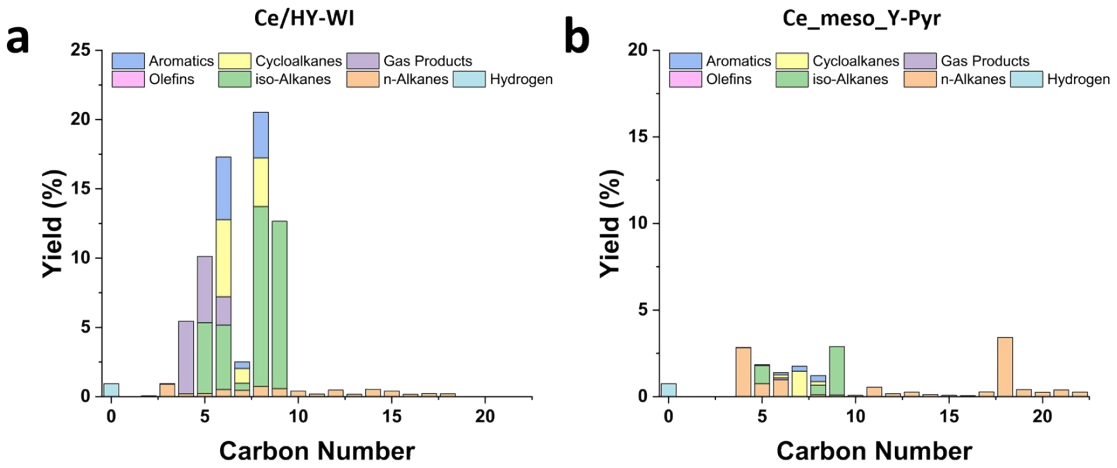

Figure S11. Product distribution from PE catalytic cracking over (a) Ce/HY-WI and (b) Ce_meso_Y-Pyr. Reaction conditions: 300°C, 4 h, atmospheric Ar, 0.1 g catalyst, and 0.2 g PE.

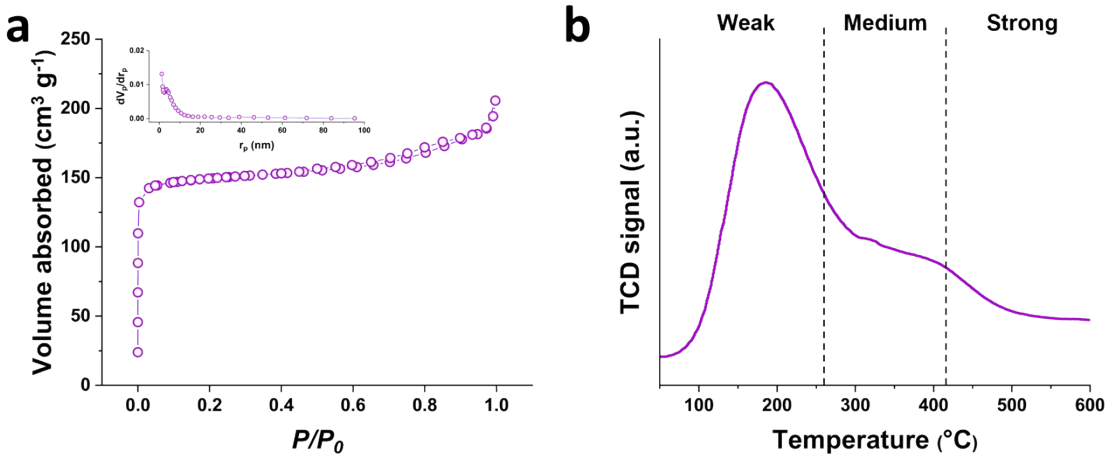

Figure S12. Physicochemical characterization of Ce/HY-WI. (a) N_2 adsorption-desorption isotherms and BJH pore size distribution of zeolites, and (b) NH_3-TPD profile.

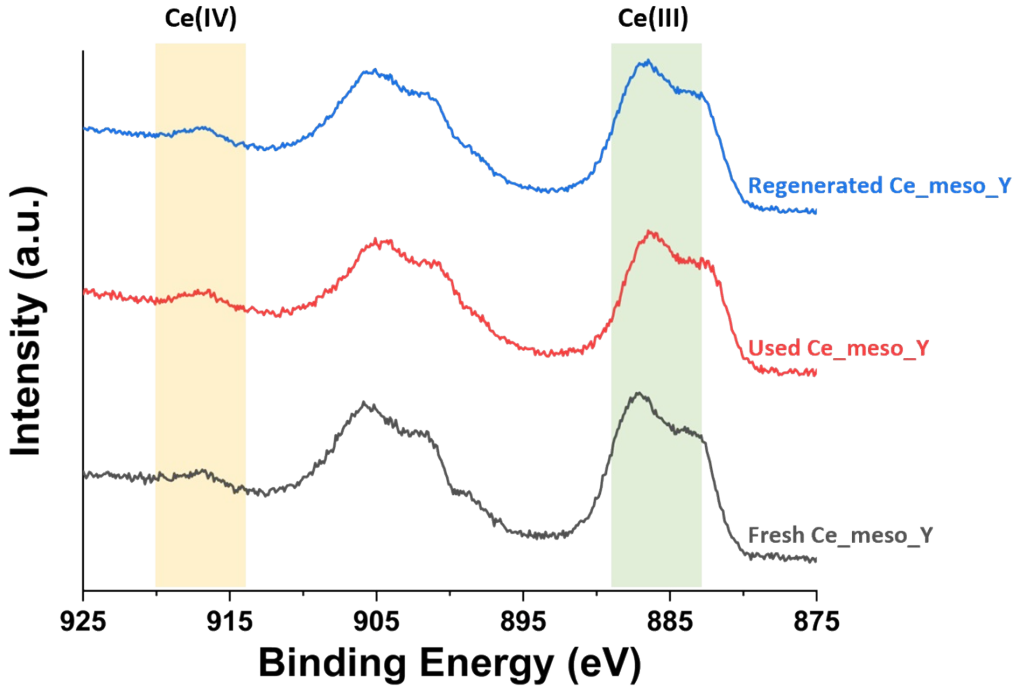

Figure S13. Ce 3d XPS spectra of fresh, used, and regenerated Ce_meso_Y catalysts.

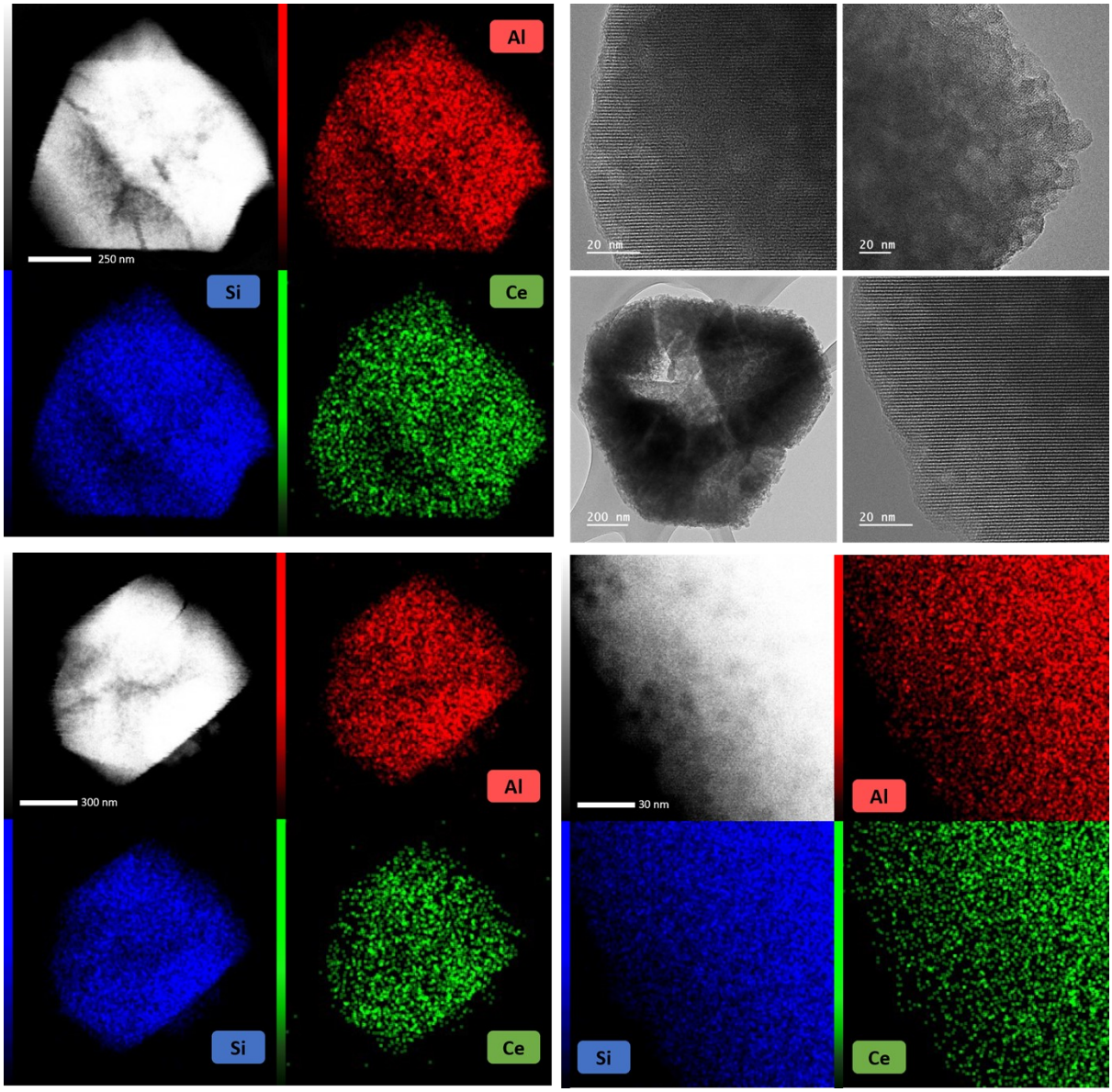

Figure S14. Representative TEM and STEM-EDX images of Ce_meso_Y.

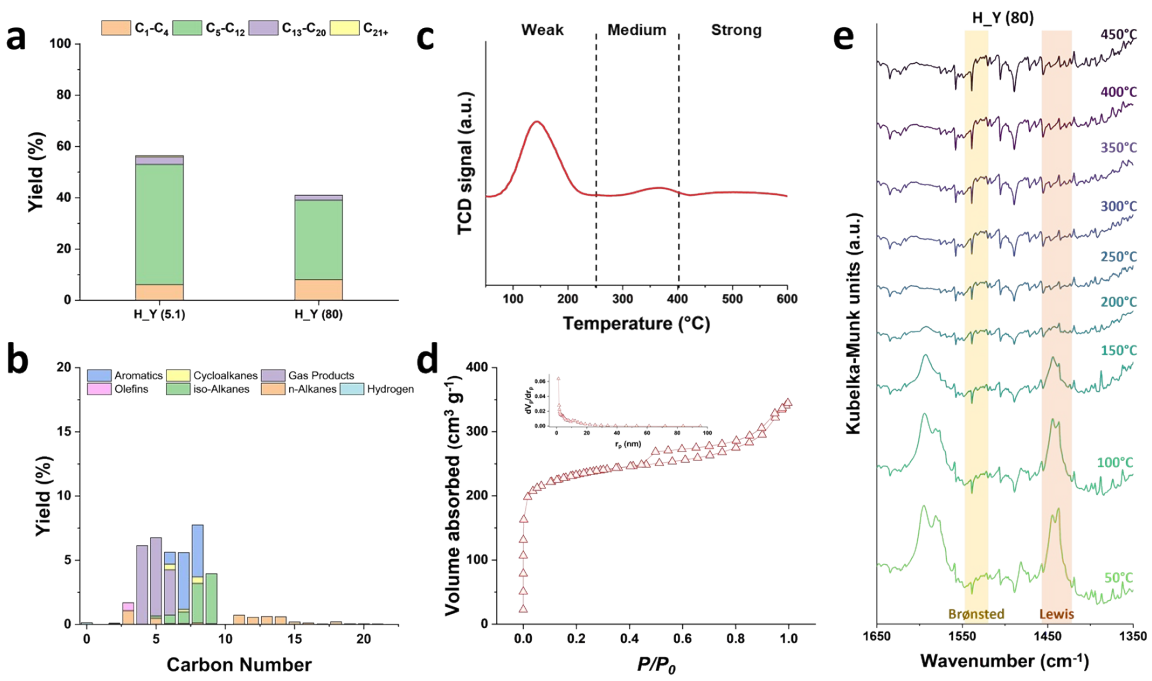

Figure S15. (a) PE catalytic cracking results over H_Y with different Si/Al ratios. (b) Product distributions for H_Y(80). Reaction conditions: 300°C, 4 h, atmospheric Ar, 0.1 g catalyst, and 0.2 g PE. (c-e) Physicochemical characterization of H_Y (80). (c) NH_3-TPD profile, (d) N_2 adsorption-desorption isotherms and BJH pore size distribution, and (e) Pyridine-DRIFTS spectra at different desorption temperatures.

Table S6. Catalytic characterization results of H_Y(80).

Catalyst	[a] Surface area ($m^2\ g^{-1}$)	[b] Pore volume ($cm^3\ g^{-1}$)	[c] Acid site density (%)			[c] Total acid site density (mmol $NH_3\ g^{-1}$)
			Weak (50-250 °C)	Medium (250-400 °C)	Strong (400-600 °C)	
H_Y(80)	580	0.527	82.1	9.2	8.7	0.79

[a] BET surface area evaluated using the standard multipoint method at $P/P_0 = 0.05–0.3$. [b] Total pore volume at $P/P_0 = 0.995$, and [c] Acid site density determined by NH_3-TPD analysis.

Table S7. Pyridine-DRIFTS analysis results of Brønsted and Lewis acid sites at different desorption temperatures.

Catalyst	At 50 °C			At 300 °C			At 450 °C		
	BAS (%)	LAS (%)	BAS/LAS	BAS (%)	LAS (%)	BAS/LAS	BAS (%)	LAS (%)	BAS/LAS
H_Y(80)	27.3	72.7	0.376	89.3	10.7	8.330	91.4	8.6	10.586

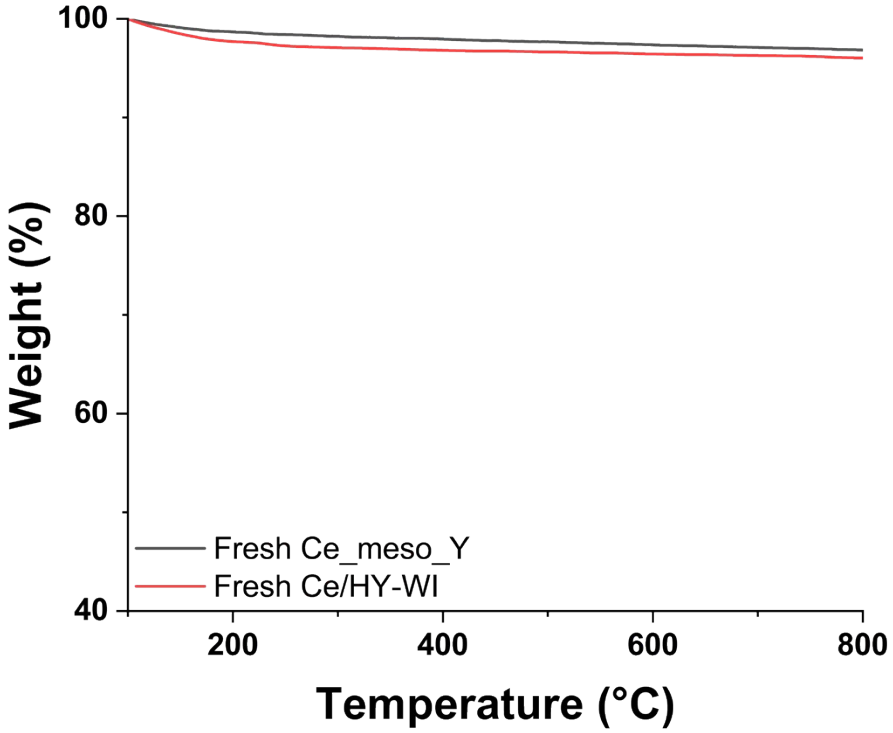

Figure S16. Thermogravimetric analysis (TGA) of fresh Ce_meso_Y and fresh Ce/HY-WI catalysts.

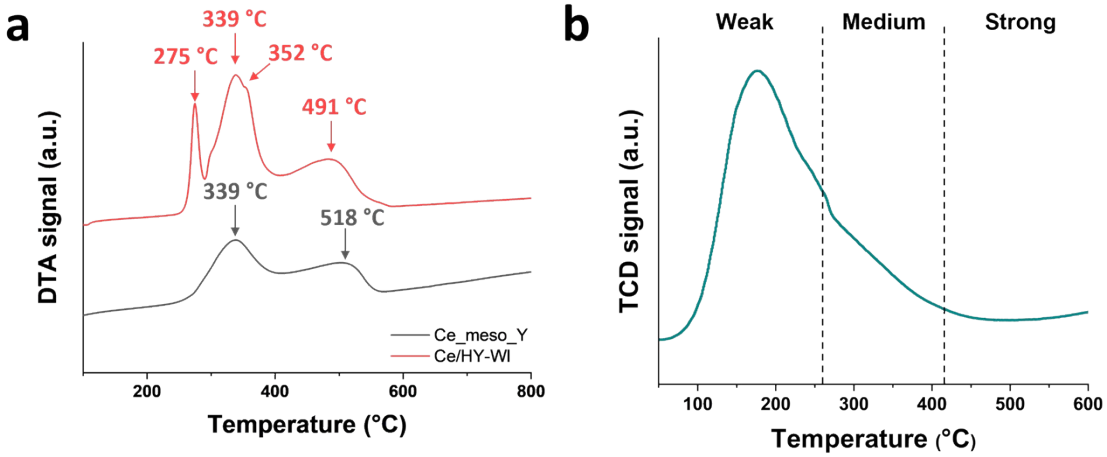

Figure S17. (a) Differential thermal analysis (DTA) of spent Ce_meso_Y and spent Ce/HY-WI catalysts. (b) NH_3-TPD profile of spent Ce_meso_Y.

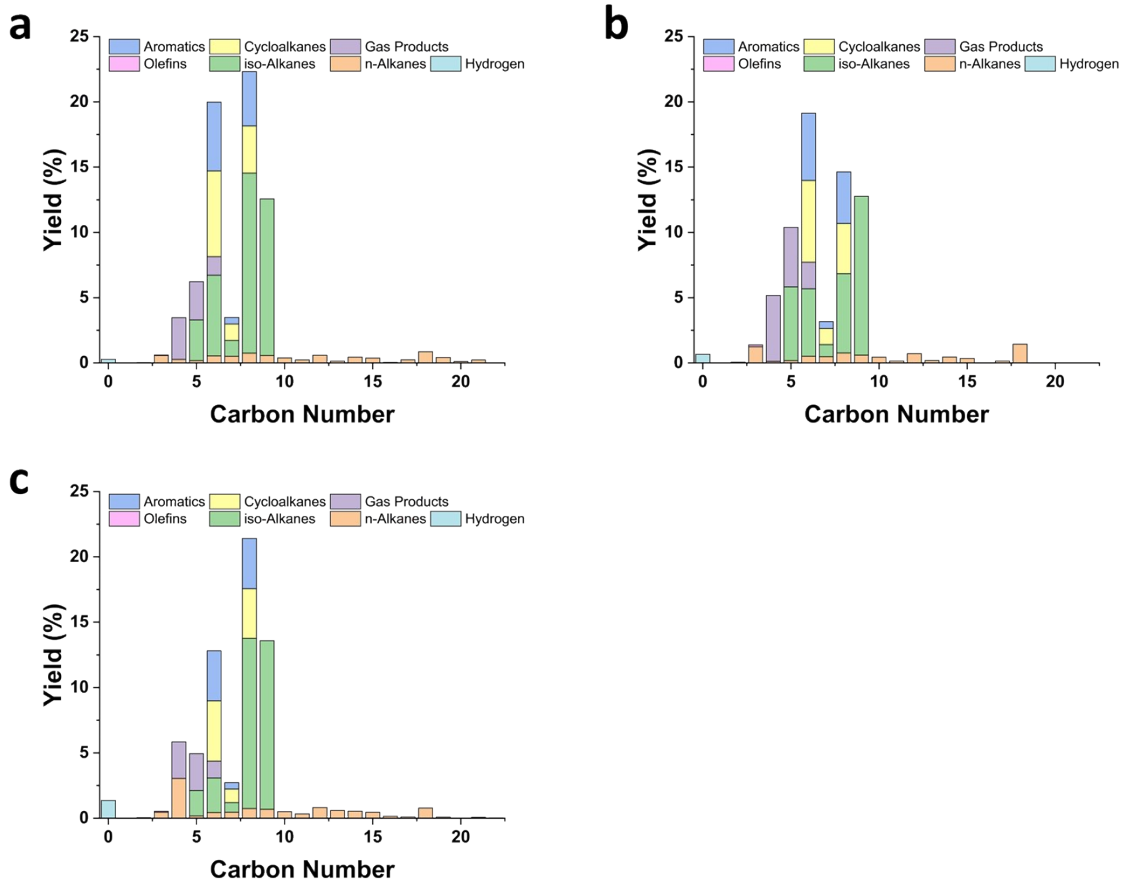

Figure S18. Product distribution from resuability test. (a) 1st reuse, (b) 2nd reuse, and (c) 3rd reuse. Reaction conditions: 300°C, 4 h, atmospheric Ar, 0.1 g catalyst, and 0.3 g PE.

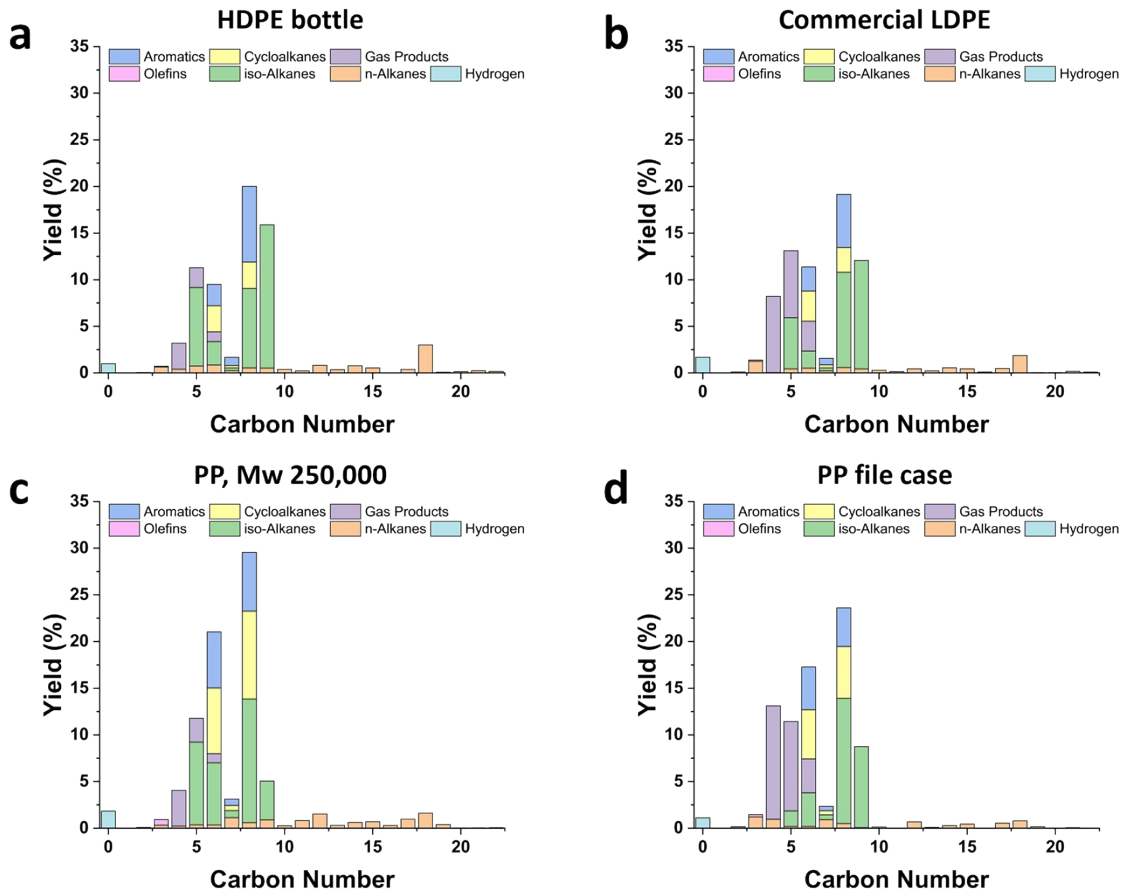

Figure S19. Product distribution from catalytic cracking reaction for post-consumer plastic wastes. (a) HDPE bottle, (b) Commercial LDPE, (c) PP, and (d) PP file case. Reaction conditions: 320 °C, 4 h, atmospheric Ar, 0.1 g catalyst, and 0.2 g reactant.

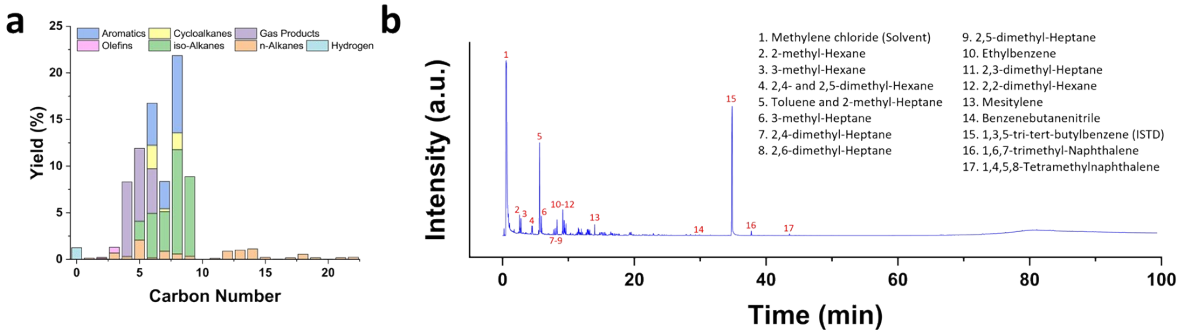

Figure S20. Product distribution from catalytic cracking reaction for mixture of PP and ABS. (a) product distributions, and (b) GC-MS analysis results.